Electronic Supplementary Material (ESI) for Journal of Materials Chemistry A.

Supplementary information

Fe^{HS} Vacancies in Prussian White Cathode Leads to Enhanced Fe^{LS} Activity and Electrode Kinetics Towards Boosted K^+ Storage

Shun Zi[#, a], Zixing Wang[#, a], Jinlong Ke[#, a], Ying Mo[a], Kexuan Wang[b], Shi Chen[b], Rui Tang[a, *], Yanhua Li[c, *], Peng Gao[a, *], Jilei Liu[a]

[a] *College of Materials Science and Engineering, Hunan Joint International Laboratory of Advanced Materials and Technology for Clean Energy, Hunan Province Key Laboratory for Advanced Carbon Materials and Applied Technology, Hunan University, Changsha 410082, China*

[b] *Joint Key Laboratory of the Ministry of Education, Institute of Applied Physics and Materials Engineering, University of Macau, Avenida da Universidade, Taipa, Macau 999078, China*

[c] *School of Materials Science and Engineering, Hunan Institute of Technology, Hengyang 421002, China*

Corresponding author. E-mail address: tangrui01@hnu.edu.cn (Rui Tang); liyanhua87@hnu.edu.cn (Yanhua Li); gaop@hnu.edu.cn (Peng Gao)

[#] S.Z., Z.X.W. and J.L.K. contributed equally to this work.

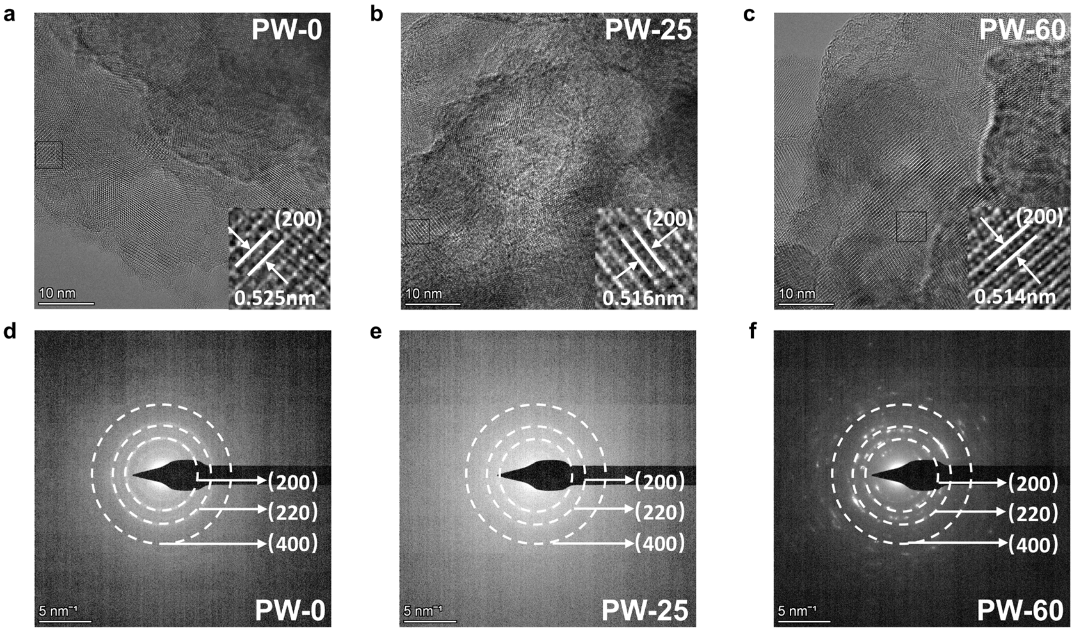

Figure S1. (a-c) HRTEM images, and (d-f) selected area electron diffractions of as-prepared three samples.

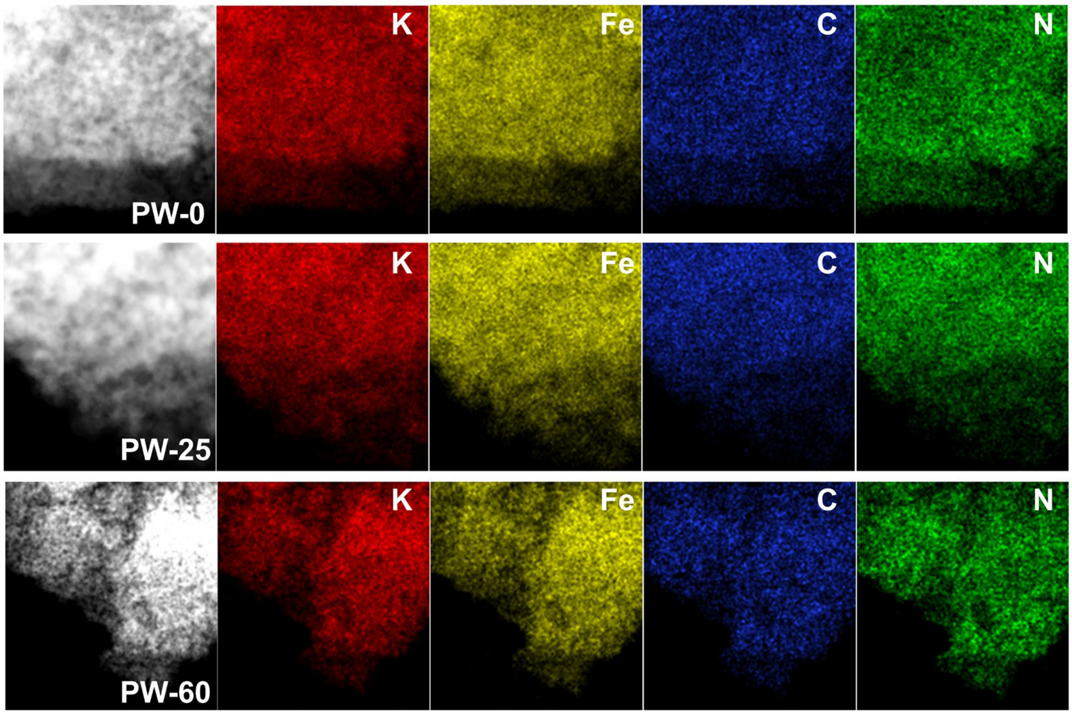

Figure S2. EDS elemental mapping images of as-prepared three samples.

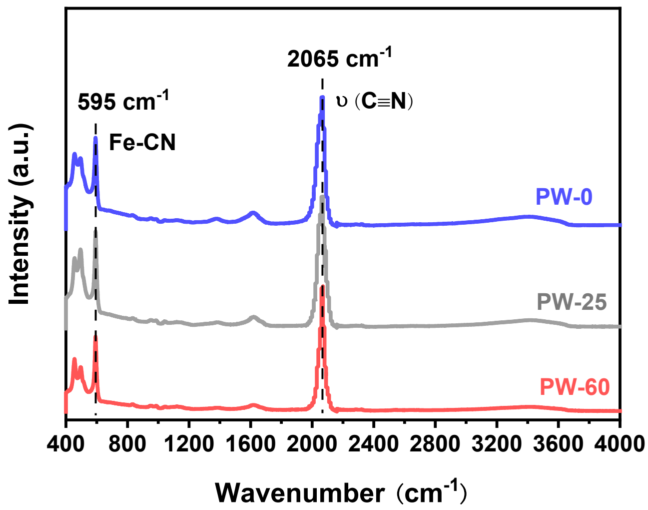

Figure S3. FTIR spectrum of PW-0, PW-25 and PW-60.

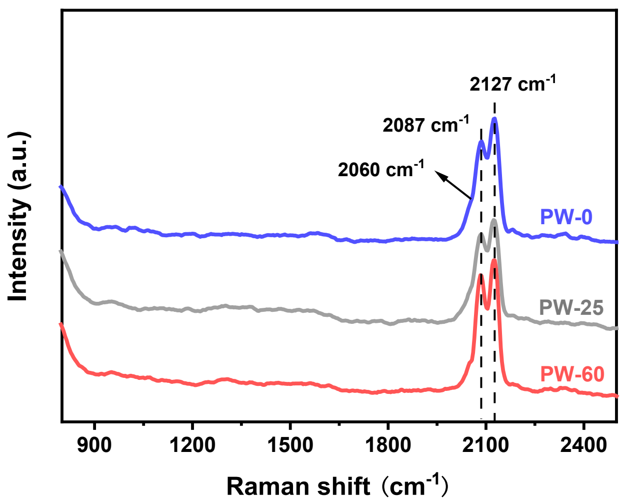

Figure S4. Raman spectrum of PW-0, PW-25 and PW-60.

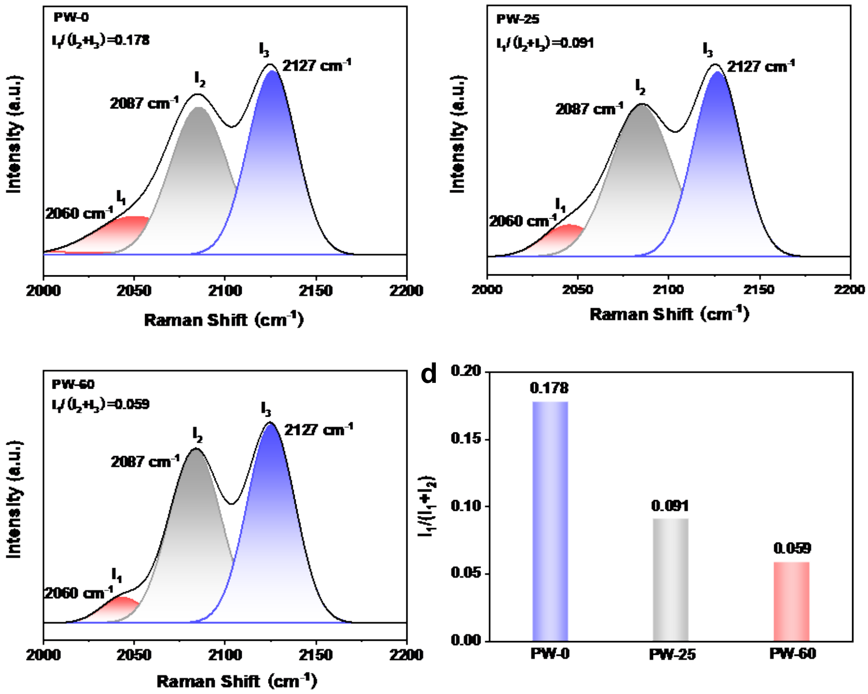

Figure S5. Raman spectra of (a) PW-0, (b) PW-25 and (c) PW-60, (d) peak area ratios (I_1/I_2+I_3) comparison.

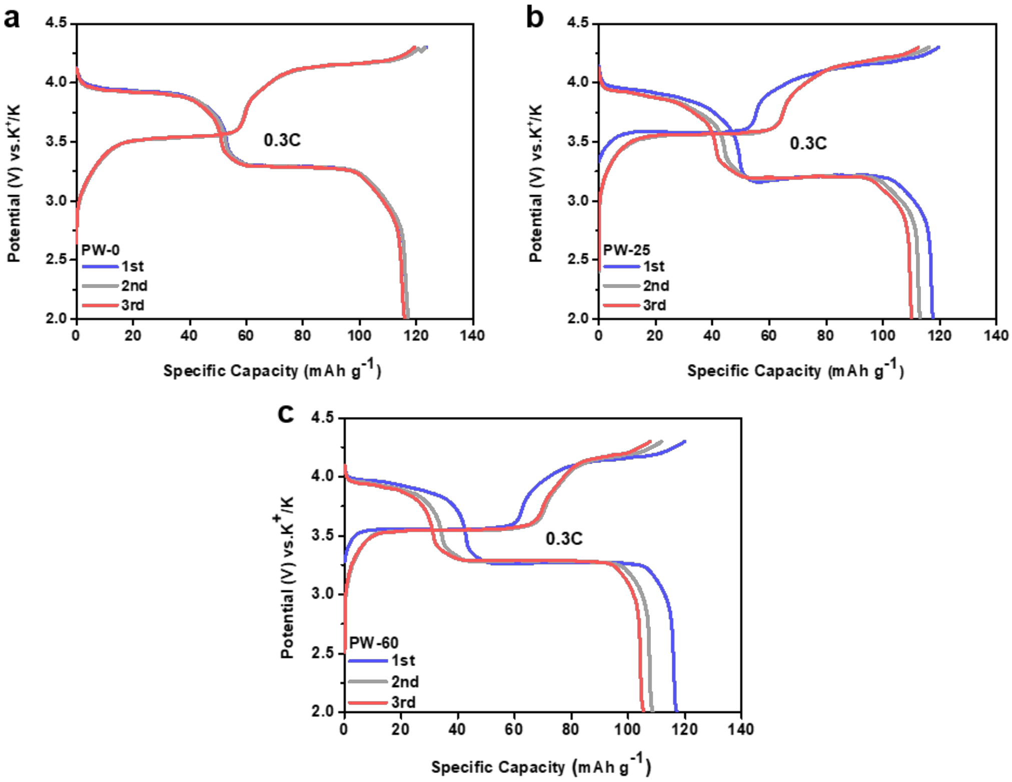

Figure S6. The first three cycles GCD curves at 0.3C of (a) PW-0, (b) PW-25 and (c) PW-60. (1C = 100 mA g^{-1})

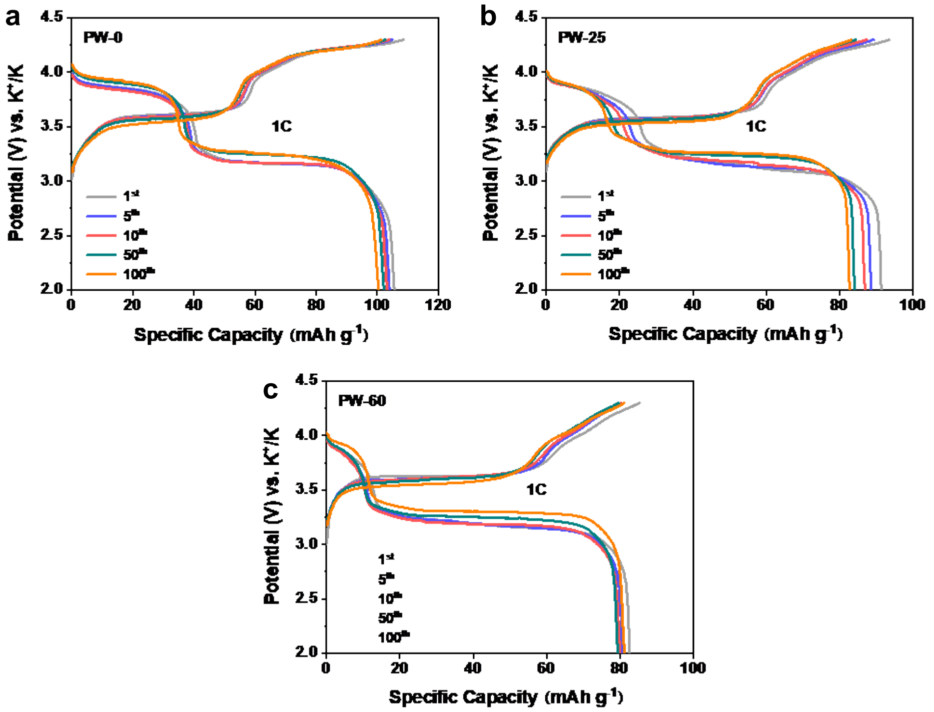

Figure S7. The 1st, 5th, 10th, 50th and 100th GCD curves at 1C of (a) PW-0, (b) PW-25 and (c) PW-60, following three cycles at 0.3C. (1C = 100 mA g^{-1})

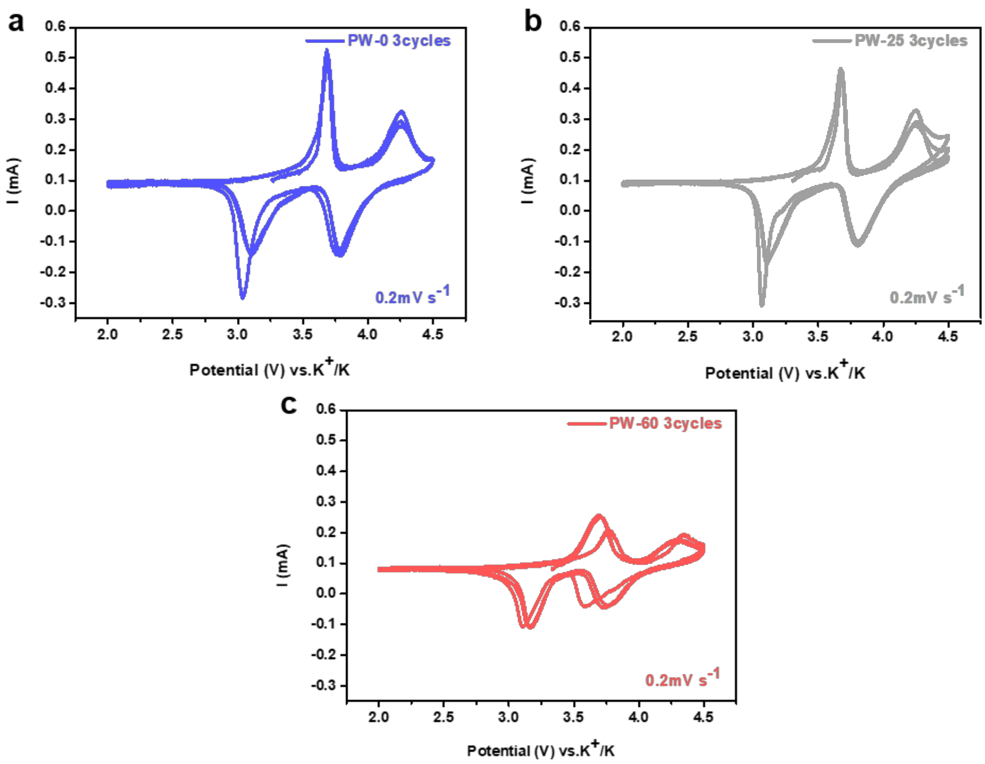

Figure S8. The first 3 cycles cyclic voltammetry curves of (a) PW-0, (b) PW-25 and (c) PW-60 at a scan rate of 0.2 mV s^{-1} within the voltage range of 2.0-4.3V (vs. K^+/K).

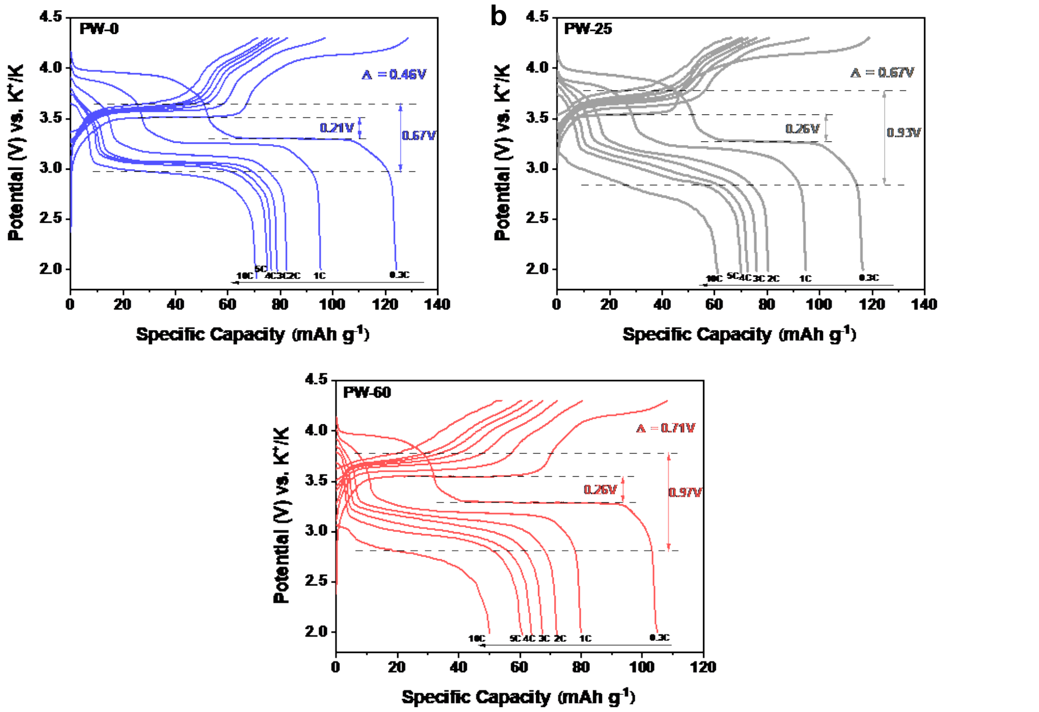

Figure S9. The GCD curves at different current densities of (a) PW-0, (b) PW-25 and (c) PW-60. (1C = 100 mA g^{-1})

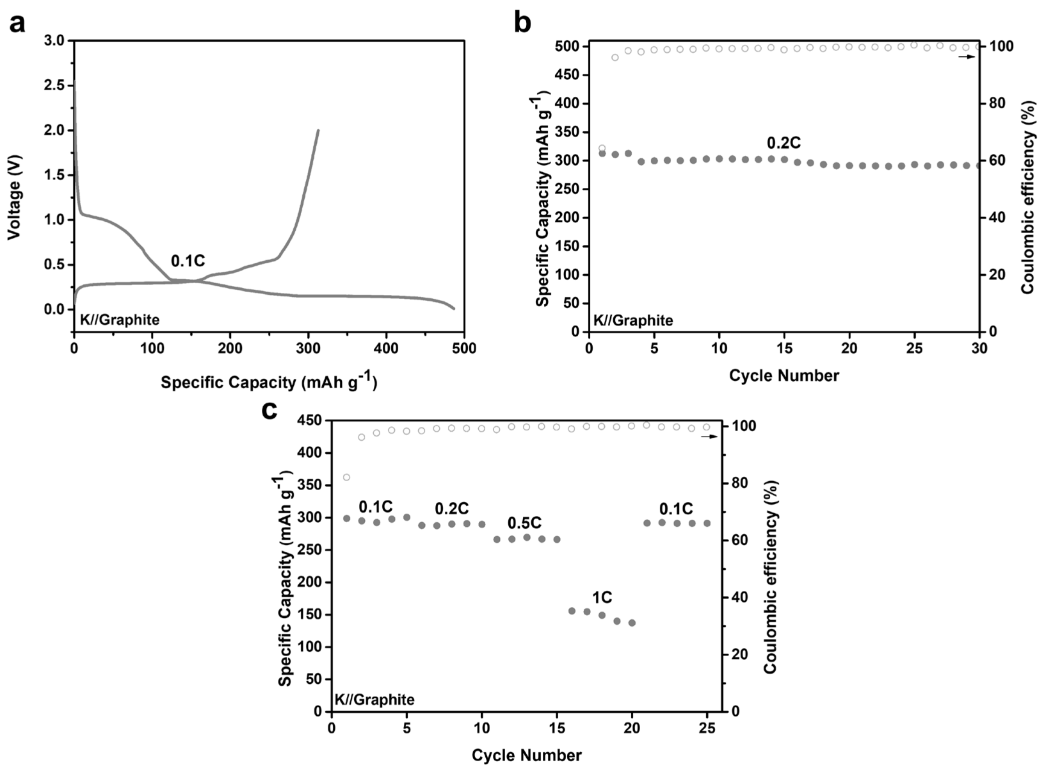

Figure S10. (a) The first galvanostatic charge-discharge profile of the K//Graphite half-cell at 0.1C, (b) The cycle performance of K//Graphite half-cell at 0.2C, (c) The rate performance of K//Graphite half-cell. (1C = 280 mA g^{-1})

Table S1. Certain parameters of full cell for PW-0.

Parameters of full cell	
N/P ratio	0.87
electrolyte amount	140 ul

Table S2. Comparison of potassium storage properties between the PW-0 and previously reported Prussian blue analogs.

Cathode material	Initial discharge capacity (mAh g^{-1}/mA g^{-1})	Capacity retention/cycle	Rate performance (mAh g^{-1}/mA g^{-1})	Reference
PW-0	93.1/100	93.1%/300	70.2/1000	This work
KMF-40	120.5/100	69.4%/100	73.2/500	1
KMF-EDTA	154.7/15	92.3%/300	74/500	2
KNiHCF	62.8/100	88.6%/100	51.1/1000	3
KNHCF	57.0/10	87.3%/1000	13.1/500	4
KFeHCF-E	77.0/25	87.6%/3200	42/1000	5
PW-HQ	113.1/50	93.0%/1000	60.4/1000	6
PB-PPY	108.6/50	~48.7%/900	35.5/500	7
KFeHCF-V	77.6/25	81.2%/50	32/200	8
KHCF@PPY	88.9/50	86.8%/500	60/1000	9
$PBN_{0.4}C_{0.6}$	86.0/20	96.9%/150	~45/200	10

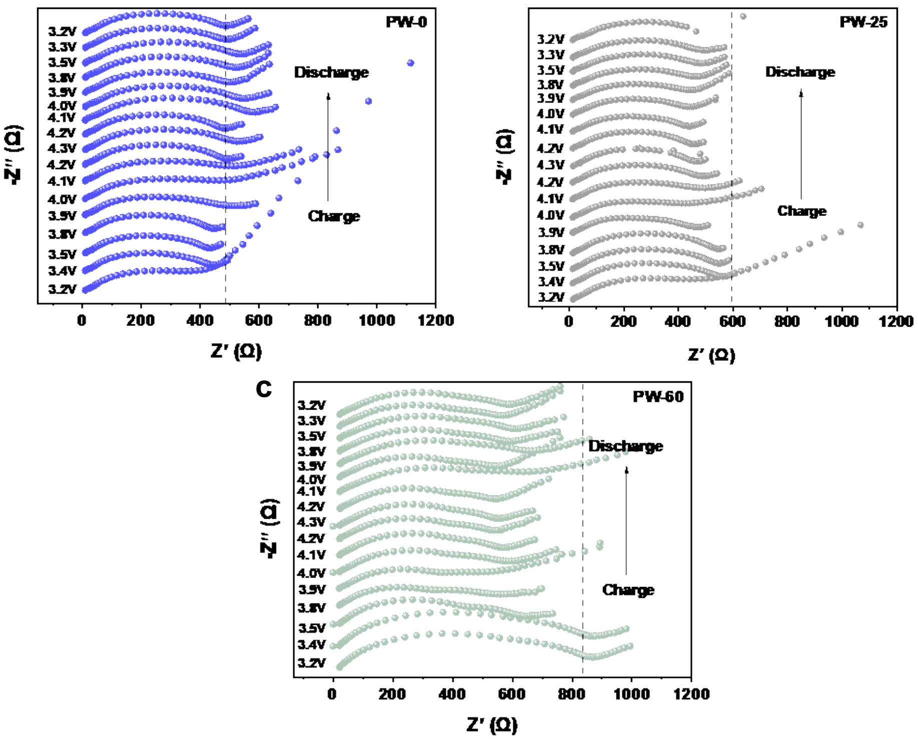

Figure S11. In-situ EIS Nyquist plots of (a) PW-0, (b) PW-25 and (c) PW-60.

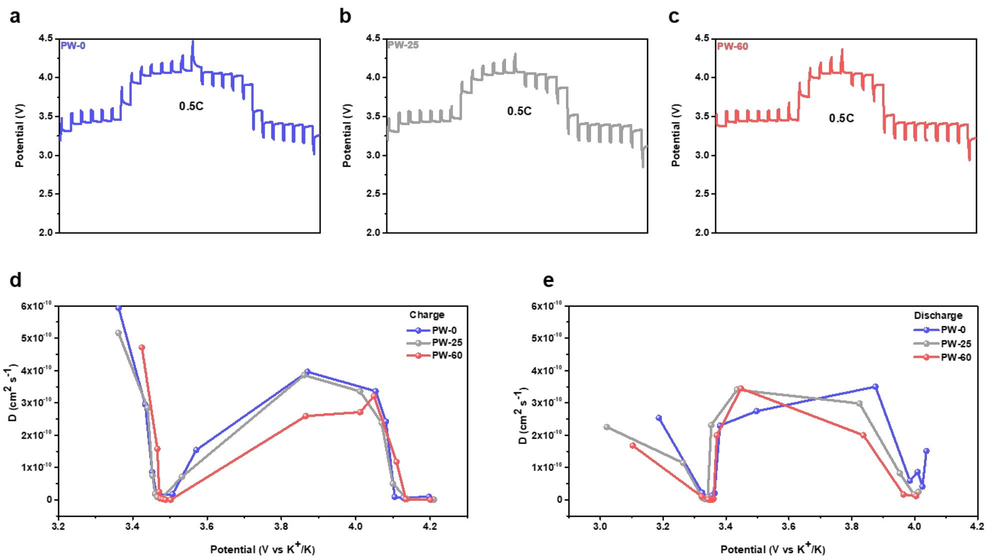

Figure S12. (a-c) The GITT curves obtained at a current density of 0.5C within the voltage range of 2.0-4.3V (vs. K^+/K), and (d-e) the calculated diffusion coefficients of PW-0, PW-25 and PW-60. (1C = 100 mA g^{-1})

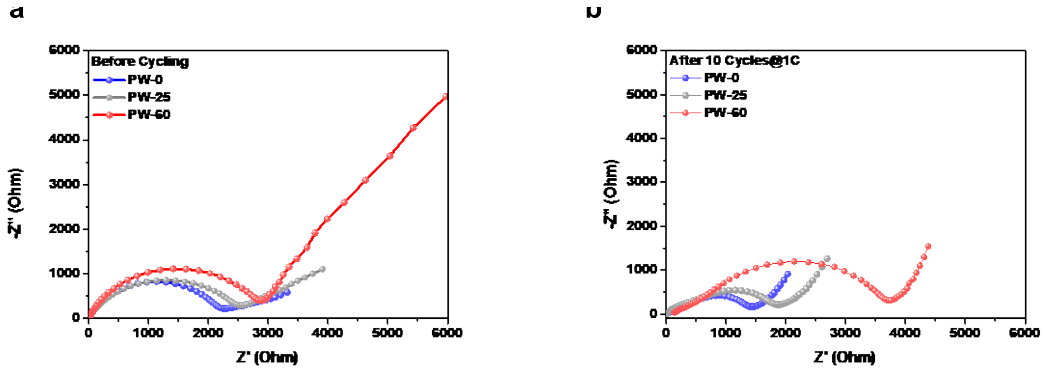

Figure S13. The Nyquist plots of (a) pristine electrodes without cycling and (b) the electrodes after ten cycles at 1C. (1C = 100 mA g^{-1})

Reference

1. W. Chen, Z. Jian, H. Li, Y. Qi, W. Jin, Y. Xia, Chinese Chemical Letters, 2021, **32**, 2433-2437.

2. L. Deng, J. Qu, X. Liu, J. Zhang, Y. Hong, M. Feng, J. Wang, M. Hu, L. Zeng, Q. Zhang, L. Guo, Y. Zhu, Nature. Communication, 2021, **12**, 2167.

3. L. Li, Z. Hu, C. Wang, Q. Zhang, S. Zhao, J. Peng, K. Zhang, S.-L. Chou, J. Chen, Angew. Chem., Int. Ed, 2021, **60**, 13050-13056.

4. S. Chong, Y. Wu, S. Guo, Y. Cao, Energy Storage Mater, 2019, **22**, 120-127.

5. W. Shu, M. Huang, L. Geng, F. Qiao, X. Wang, Small, 2023, **19**, 2207080.

6. R. Ma, Z. Wang, Q. Fu, W. Zhou, Y. Mo, J. Tu, Z. Wang, P. Gao, C. Fan, J. Liu, J. Energy Chem, 2023, **83**, 16-23.

7. M. Zhou, X, Tian, Y. Sun, X. He, H. Li, T. Ma, Q. Zhao, J. Qiu, Nano Res, 2023, **16**, 6326-6333.

8. Z. Wang, W. Zhuo, J. Li, L. Ma, S. Tan, G. Zhang, H. Yin, W. Qin, H. Wang, L. Pan, A. Qin, W. Mai, Nano Energy, 2022, **98**, 107243.

9. Q. Xue, L. Li, Y. Huang, R. Huang, F. Wu, R. Chen, ACS Appl. Mater. Interfaces 2019, **11**, 22339-22345.

10. B. Huang, Y. Shao, Y. Liu, Z. Lu, X. Lu, S. Liao, ACS Appl. Energy Mater, 2019, **2**, 6528-6535.